Geospatial Health 2023; volume 18:1189

Spatiotemporal distribution and geostatistically interpolated mapping of the melioidosis risk in an endemic zone in Thailand

Jaruwan Wongbutdee, Jutharat Jittimanee, Wacharapong Saengnill

Geospatial Health Research Group, College of Medicine and Public Health, Ubon Ratchathani University, Thailand

Abstract

Melioidosis, a bacterial, infectious disease contracted from contaminated soil or water, is a public health problem identified in tropical regions and endemic several regions of Thailand. Surveillance and prevention are important for determining its distribution patterns and mapping its risk, which have been analysed in the present study. Case reports in Thailand were collected from 1 January 2016 to 31 December 2020. Spatial autocorrelation was analyzed using Moran's *I* and univariate local Moran's *I*. Spatial point data of melioidosis incidence were calculated, with risk-mapping interpolation performed by Kriging. It was highest in 2016, at 32.37 cases per 100,000 people, and lowest in 2020, at 10.83 cases per 100,000 people. General observations revealed that its incidence decreased slightly from 2016 to 2018 and drastically in 2019 and 2020. The Moran's *I* values for melioidosis incidence exhibited a random spatial pattern in 2016 and clustered distribution from 2017 to 2020. The risk and variance maps show interval values. These findings may contribute to the monitoring and surveillance of melioidosis outbreaks.

Correspondence: Wacharapong Saengnill, College of Medicine and Public Health, Ubon Ratchathani University, 34190, Warin Chamrap, UbonRatchathani, Thailand.
Tel.: +66.995451635 - Fax: +66.45353901
E-mail: watcharapong.s@ubu.ac.th

Key words: melioidosis, interpolated mapping, spatial autocorrelation, Burkholderia pseudomallei Thailand.

Contributions: JW and JJ collected data and critically revised the manuscript for content. JW and WS designed the study. WS analyzed spatial data and write the manuscript. All authors read and approved the final manuscript.

Conflict of interest: the authors declare no potential conflict of interest, and all authors confirm accuracy.

Availability of data and materials: all data generated or analyzed during this study are included in this published article.

Ethics approval: the protocol for research on humans was approved by the Ubon Ratchathani University Human Research Ethics Committee (Approval ID: UBU-REC-128/2563).

Acknowledgements: this research was supported by Grants from College of Medicine and Public Health, UbonRatchathani University.

Received: 25 January 2023.
Accepted: 21 June 2023.

Geospatial Health 2023; 18:1189
doi:10.4081/gh.2023.1189

Introduction

Melioidosis is an infectious disease contracted from soil or water contaminated by the bacterium *Burkholderia pseudomallei.* These bacteria have been identified in various water resources, including public tap water, as well as in soil within the depth range of 0-90 cm (Limmathurotsakul *et al*., 2013; Thaipadungpanit *et al*., 2014). Apart from infection via drinking infected water, the bacteria can enter the human body through the skin or wounds or via inhalation of dust particles. High fever, mucus cough, chest pain, with pus in the lungs, liver or spleen are common symptoms of melioidosis. Severe cases can lead to organ failure and death. Several studies have performed experiments and analyzed factors influencing the environmental sustainability of *B. pseudomallei* growth, such as soil moisture, low soil pH, clay-loam soil and temperatures of 37-42°C (Kaestli *et al*., 2009; Limmathurotsakul *et al*., 2013; Paksanont *et al*., 2018; Palasatien *et al*., 2008). These are reveal key factors for *B. pseudomallei* survival and tolerance in the environment, which may increase the opportunity of melioidosis infection in humans.

Melioidosis has been identified in tropical regions and particularly in Thailand, where it is endemic, with reported incidences of 4.07, 4.24, and 4.21 cases per 100,000 people in 2018, 2019 and 2020, respectively (Bureau of Epidemiology, 2023). The bacterium has been identified in paddy soil, disused land and water supplies (Finkelstein *et al*., 2000; Limmathurotsakul *et al*., 2013; Saengnill *et al*., 2020; Wang-Ngarm *et al*., 2014). Several studies on its clinical epidemiology and increasing incidence in humans in north-eastern Thailand and neighbouring countries, *e.g.*, Laos have provided an important basis of knowledge for future research (Chen *et al*., 2012; Dance *et al*., 2018; Hantrakun *et al*., 2019; Limmathurotsakul *et al*., 2010). However, melioidosis prevention and control may necessitate the application of spatial and temporal information to identify the disease and to map its distribution accurately. Most medical reports have not yet integrated spatial

data. Therefore, methods based on geographic information systems (GIS) are essential for the collection, management, analysis and visualization of spatial data at specific locations. GIS, a powerful tool for spatial statistical analysis, has been successfully applied in spatial epidemiology and public health, for instance via space-time scanning to detect emerging clusters and for spatiotemporal monitoring (Kulldorff, 1997). Importantly though, small-cluster zones can be hidden when particularly large maximum scanning windows are used (Han *et al*., 2016). The most popular spatial approaches use the global or local Moran's *I* statistic for the analysis of spatial autocorrelation. This method focuses on cluster and outlier locations to reveal differences in spatial dependence, assuming that points are most similar to their neighbors. It has been applied to analyze spatial dependence in order to identify the distribution of *B. pseudomallei* (Rachlin *et al*., 2020). Spatial autocorrelation analysis has been used to interpret the melioidosis incidence in Taiwan and suburban Australia (Corkeron *et al*., 2010; Dai *et al*., 2012). However, because few studies have focussed on its spatiotemporal distribution and spatial autocorrelation, information on its disease transmission is still lacking.

This study aimed to analyse the spatial autocorrelation and spatial pattern of melioidosis risk, and to create incidence risk maps by applying geostatistics, a quantitative field within GIS, an approach that can analyse variance in distance from sampling points and also calculate spatial correlations for single variables, where closer points are considered more similar. Geostatistical tools have been used to map the probability of disease occurrence by determining the lag distances between sites (paddy fields) positive for *B. pseudomallei* (Limmathurotsakul *et al*., 2010; Saengnill *et al*., 2020). We used a semivariograms to determine the spatial autocorrelation of the lag distances, and indicator Kriging interpolation to generate the risk map of melioidosis incidence.

Materials and Methods

Design and study site

The study area was Ubon Ratchathani Province, with its 25 districts and 219 sub-districts. It partly borders Laos and Cambodia in lower, north-eastern Thailand. A retrospective study of secondary data was designed to monitor the temporal dynamics of melioidosis incidence over the five-year period from 2016 to 2020. Medical data such as case reports do not provide sufficient information for disease prevention and control. We therefore used GIS to collect, manipulate and visualize the spatiotemporal data to assist analyses of spatial autocorrelation to reveal melioidosis distribution in terms of clustering, dispersion and random patterns. This was done to identify high-risk areas based on the relationship between spatial and attribute data and to develop a geostatistical model of melioidosis distribution. Semivariogram and indicator Kriging was applied to map the melioidosis risk and determine the lag distances between cases. The protocol for research on humans was approved by the Ubon Ratchathani University Human Research Ethics Committee (Approval ID: UBU-REC-128/2563).

Data collection

This study used melioidosis cases reported from 1 January 2016 to 31 December 2020 at Sunpasitthiprasong Hospital (Ubon Ratchathani Province). The 1,901 cases reported showed a lowering trend over the study period (Table 1). The cases in each subdistrict were aggregated by subdistrict code. The population data for 2016–2020 were obtained from the official statistical registration system of the Department of Local Administration. The coordinate reference system was the spheroid datum of WGS 1948 and UTM zone 48N.

Data preparation and analysis

The data were recorded, manipulated, processed, and converted into comma-separated value (CSV) format using a Microsoft Excel Worksheet (.xlsx format). QGIS was used to generate the spatial data and to join the attribute tables via a one-to-one relationship between the spatial data and attribute data, using sub-district code as the primary key. For each sub-district, the melioidosis incidence was calculated by dividing the number of cases by that of the population and multiplying the result by 10,000.

Spatial autocorrelation was analyzed using Moran's *I* and univariate local Moran's *I* by GEODA software. Feature point centroids, indicating the centres of the sub-district boundaries, were created from the X and Y coordinates, with incidence spatial point data for each year transformed from ratio data into binary data. For melioidosis incidence >0,1 was assigned; for incidence = 0,0 was assigned. The R gstat package was used for spatial and geostatistical modelling and prediction. Spatial autocorrelation was determined using a semivariogram and interpolated the mapping of melioidosis risk was done by indicator Kriging.

Spatial autocorrelation

Spatial autocorrelation concerns the similarity between two or more observation values. The correlations of the objects are measured using a set of locations dependent on values of the nearest variable at other locations. Objects that are not correlated or are more distant are considered dissimilar. Spatial autocorrelation often reveals distribution patterns such as clustering, dispersion and random distribution.

We used global Moran's *I* statistic to estimate the potential correlation of melioidosis incidence considering queen contiguity-

Table 1. Global Moran's *I* of melioidosis incidence during 2016-2020.

Year	Case (no.)	Moran's *I*	*z*-score	SD	p	Pattern
2016	577	–0.011	–0.223	0.034	0.462	Random
2017	523	0.059	1.706	0.039	0.058	Cluster
2018	402	0.156	3.763	0.042	0.002	Cluster
2019	210	0.135	3.344	0.041	0.003	Cluster
2020	189	0.091	2.283	0.041	0.023	Cluster

SD, standard deviation; Spatial significance at pseudo p<0.05.

base weights, which share a common boundary edge between two spatial units. Therefore, the spatial weight of the neighbouring relationship was assigned values of 1or 0. Moran's *I* ranges from −1 to 1. A positive value indicates a clustered pattern and negative autocorrelation implies dispersion. Zero (no autocorrelation) indicates a random distribution. Findings were considered statistically significant at p<0.05. Moran's *I* was calculated as:

$$I = \frac{N}{\sum_i \sum_j w_{ij}} \frac{\sum_i \sum_j w_{ij} (x_i - \bar{x})(x_j - \bar{x})}{\sum_i (x_i - \bar{x})^2} \quad \text{Eq. 1}$$

where N is the number of observations; x_i and x_j the observed values for features i and j; and w_{ij} the spatial weight at locations i and j.

We used local Moran's *I* to identify hotspots, coldspots and spatial outliers. Using local Moran's *I*, features that have neighbours with high or low values are given positive values; if the neighbour's *I* value indicates dissimilarity, the feature is given a negative value. The *z*-score and *p*-value reveal the null hypothesis used to accept significance and the output feature class for spatial dependency. Cluster and outlier detection were performed based on four types of autocorrelation: i) hotspots that signify neighbouring zones with high *I* values (HH); ii) coldspots that signify neighbouring zones with low *I* values (LL); iii) a zone with a high *I* value surrounded by zones with low *I* values (HL); and iv) a zone with low *I* value surrounded by zones with high values (LH). The equations used were:

$$I_i = \frac{x_i - \bar{x}}{s_i^2} \sum_{j=1, j \neq i}^{n} w_{ij} (x_i - \bar{x}) \quad \text{Eq. 2}$$

where s_i^2 is the variance:

$$s_i^2 = \frac{\sum_{j=1}^{n} w_{ij}}{(n-1)} - \bar{x}^2 \quad \text{Eq. 3}$$

Geostatistics

Geostatistics is a powerful tool for describing spatial dependency based on the spatial autocorrelation of neighbouring observation points. A continuous surface can be interpolated from the measured locations to obtain probability predictions for each location. The sub-district centroids therefore represent similar attributes of melioidosis distribution. The lag distance, the distance in statistical space in the variogram cloud (Eq. 4) represents half the mean squared difference between each pair of sub-district melioidosis values (the output of each sample of matching data points). A semivariogram function was fit according to three parameters: i) the sill, which represents the total variance at which the spatial autocorrelation appears to level off; ii) the nugget, which represents the small separation distance or measurement error during sampling; and iii) the range, which defines the distance within which points are considered to be spatially correlated. The empirical semivariogram was used to examine the spatial relationships using spherical, exponential and Gaussian models. To select the best-fit model, it was necessary to evaluate the melioidosis predictions. Therefore, we evaluated model fit based on the mean absolute error and root mean square error (RMSE).

$$Y(h) = \frac{1}{2N(h)} \sum_{i=1}^{N(h)} [z(x_i + h) - z(x_i)]^2 \quad \text{Eq. 4}$$

where $N(h)$ is the number of sample pairs at location h and $z(x_i)$ with $z(x_i + h)$ the values of the variables at location x_i and at the location separated by distance h, respectively.

Spatial autocorrelation, the weight that relates each point and distance, is determined by a semivariogram. We interpolated the unknown values to achieve continuous mapping of the melioidosis distribution via indicator Kriging to map the probabilities of the presence and absence of melioidosis. Incidence was classified as binary (presence = 1, absence = 0); an incidence >0 was assigned 1, and an incidence of 0 was assigned 0. Indicator Kriging was used to predict the risk distribution and uncertainty surfaces, where higher values than 0-1indicate the potential of a melioidosis outbreak. Calculations were done by the equation:

$$I(x_i : z_k) = \{1, \ if \ z(x) > z_k, otherwise \ 0\} \quad \text{Eq. 5}$$

where $z(x)$ is the melioidosis incidence and z_k the threshold based on from this incidence.

Validation

To examine the error association between the predicted and actual values and thus evaluate the model's accuracy, the melioidosis prediction map was cross-validated to. Leave-one-out cross validation (LOOCV) was used to evaluate model performance. This involves the use of all values to estimate the test error; one value is left out of the data set for testing, and the remaining values make up the training data for the prediction model. The mean absolute error (MAE) is the absolute difference between the observation and prediction values, while the RMSE measures the prediction quality, providing the average of the squared differences between observations and predictions. MAE and RMSE were calculated as follows:

$$\text{MAE} = \frac{1}{n} \sum_{i=1}^{n} |(y_i - \hat{y}_i)| \quad \text{Eq. 6}$$

$$\text{RMSE} = \sqrt{\frac{1}{n} \sum_{i=1}^{n} [(y_i - \hat{y}_i)^2} \quad \text{Eq. 7}$$

where n is the sample size; y_i the observed value at location I; and $\hat{y}_i$ the predicted value of observation i.

Results

At 32.37 cases of melioidosis per 100,000 people, the incidence in Ubon Ratchathani Province was the highest in 2016 and reached the lowest value in 2020 (10.83 cases per 100,000 people). Overall, the incidence decreased slightly from 2016 to 2018 and drastically so in 2019 and 2020 (Figure 1). The monthly incidence trend for the study period gives the outbreak frequency and reveals that melioidosis is an endemic disease (Figure 2). Incidence

decreased slightly over the period, and no cases were observed in November 2019; however, as can be seen in Figure 2, the trend was not comprehensive. The cumulative number of cases for each year did does not differ monthly. These findings indicate that melioidosis is reported in all seasons in Thailand.

Spatial and temporal distributions of the melioidosis incidence per 10,000 people in each sub-district were generated via quantile classification (Figure 3). The highest incidence was 66.89 cases per 10,000 people in 2016, while all other years had >10 cases per 10,000 people. Figure 3 reveals that outbreaks were frequent in the northern regions and occasional in the southern regions. Spatial autocorrelation was determined by identifying the pattern in the distribution. Table 1 presents the Moran's *I* values for melioidosis incidence: the spatial distribution for 2016 exhibits a random distribution (I=−0.011, p=0.462), whereas clustering was revealed for 2017–2020. The maps of melioidosis incidence in the study area show spatial hotspots and significance (Figures 4 and 5). They reveal clusters of sub-districts and also sub-district outliers. For 2018, the hotspots (HH zones) occurred mostly in the northern and central parts of the study area. For the years 2016, 2017, 2018, 2019 and 2020, the numbers of sub-districts classified as hotspots were 6, 8, 12, 13, and 10, respectively. Based on the spatial autocorrelation, determined using the empirical semivariogram, locations closer locations exhibited higher similarity in terms of melioidosis incidence. The minimum ranges were 38.03 and 44.69 km for 2017 and 2019, respectively; the highest range (116.91 km) was obtained for 2020. The nugget and sill values and the values used for cross-validation are shown in Table 2.

Figures 6 and 7 provide the probability and variance maps of melioidosis incidence.

Melioidosis occurred often in the northern region, and rarely in the central and southern regions, of the Ubon Ratchathani Province (Figures 6 and 7). Disease outbreak monitoring and evaluation often depends on prevalence and incidence values during the same time-period. Here, we visualized melioidosis incidence spatially, revealing spatial autocorrelation with both clustered and random distributions (Table 1). In 2016, the distribution of melioidosis was random, indicating a non-uniform distribution and reflecting uncertainty in the numbers of melioidosis cases.

Figure 1. Melioidosis incidence in 2016-2020.

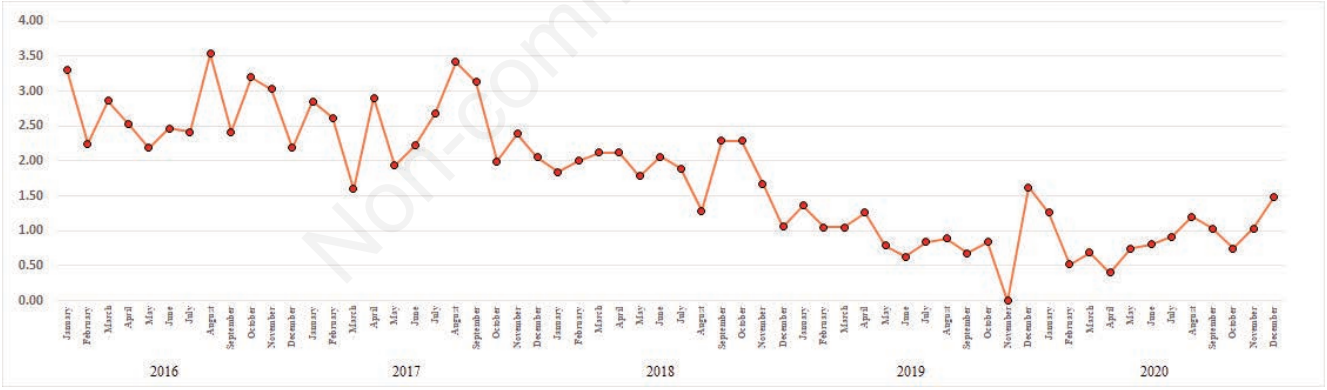

Figure 2. Trend of monthly melioidosis outbreaks in 2016-2020.

Table 2. Semivariogram model and cross validation.

Year	Expression	Nugget	Sill	Range (km)	MAE	RMSE
2016	Spherical	0.159	0.038	62.42	0.361	0.427
2017	Exponential	0.224	0.014	38.03	0.461	0.482
2018	Spherical	0.214	0.038	61.47	0.460	0.480
2019	Gaussian	0.236	0.018	44.69	0.482	0.489
2020	Exponential	0.224	0.009	116.91	0.463	0.479

Nugget, the value at which the semi-variogram (almost) intercepts the y-value; Sill, the value at which the model first flattens out; Range, the distance at which the model first flattens out; MAE, mean absolute error; RMSE, root mean square error.

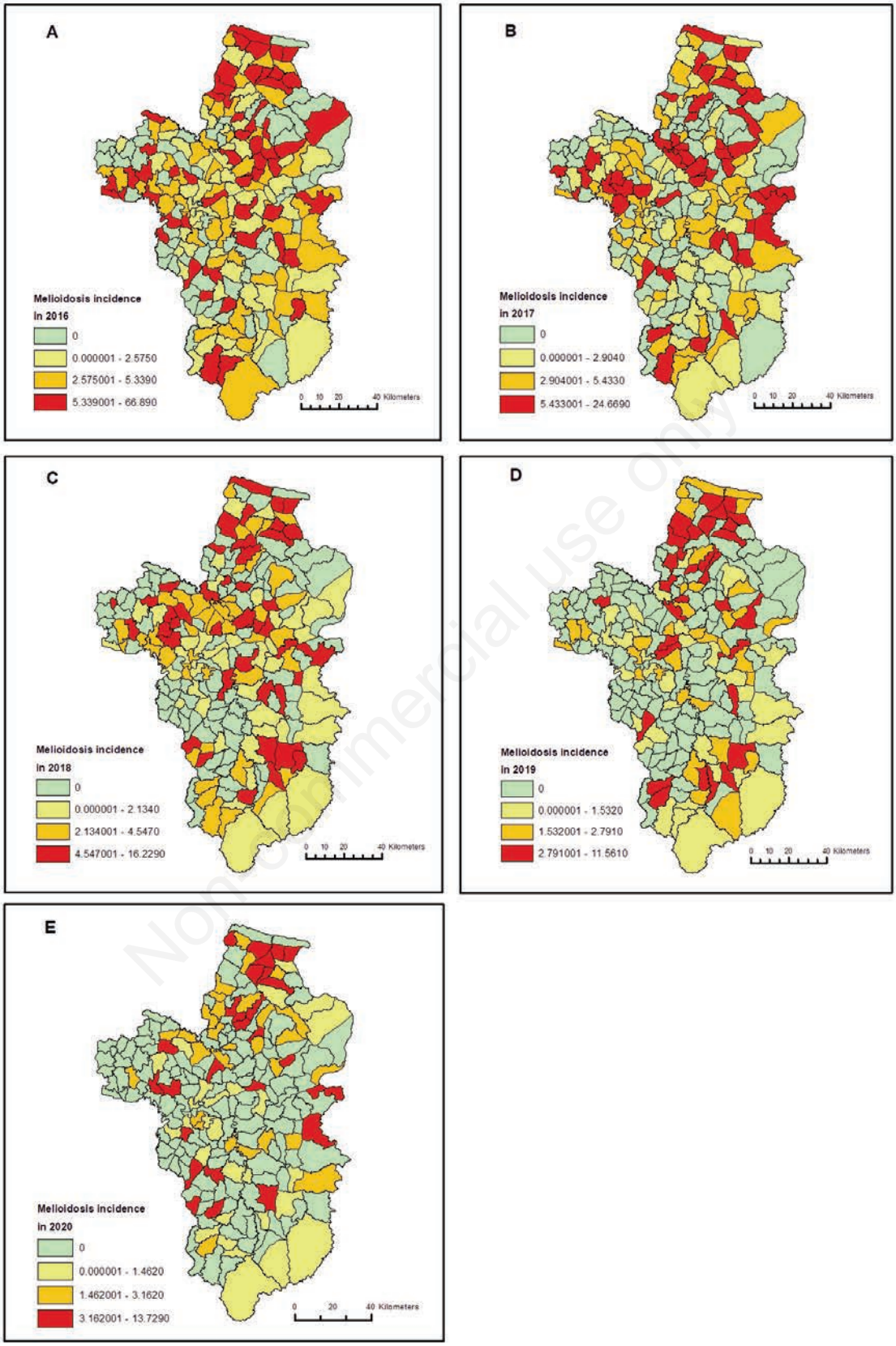

Figure 3. Spatial distribution of melioidosis incidence. A) 2016; B) 2017; C) 2018; D) 2019; E) 2020.

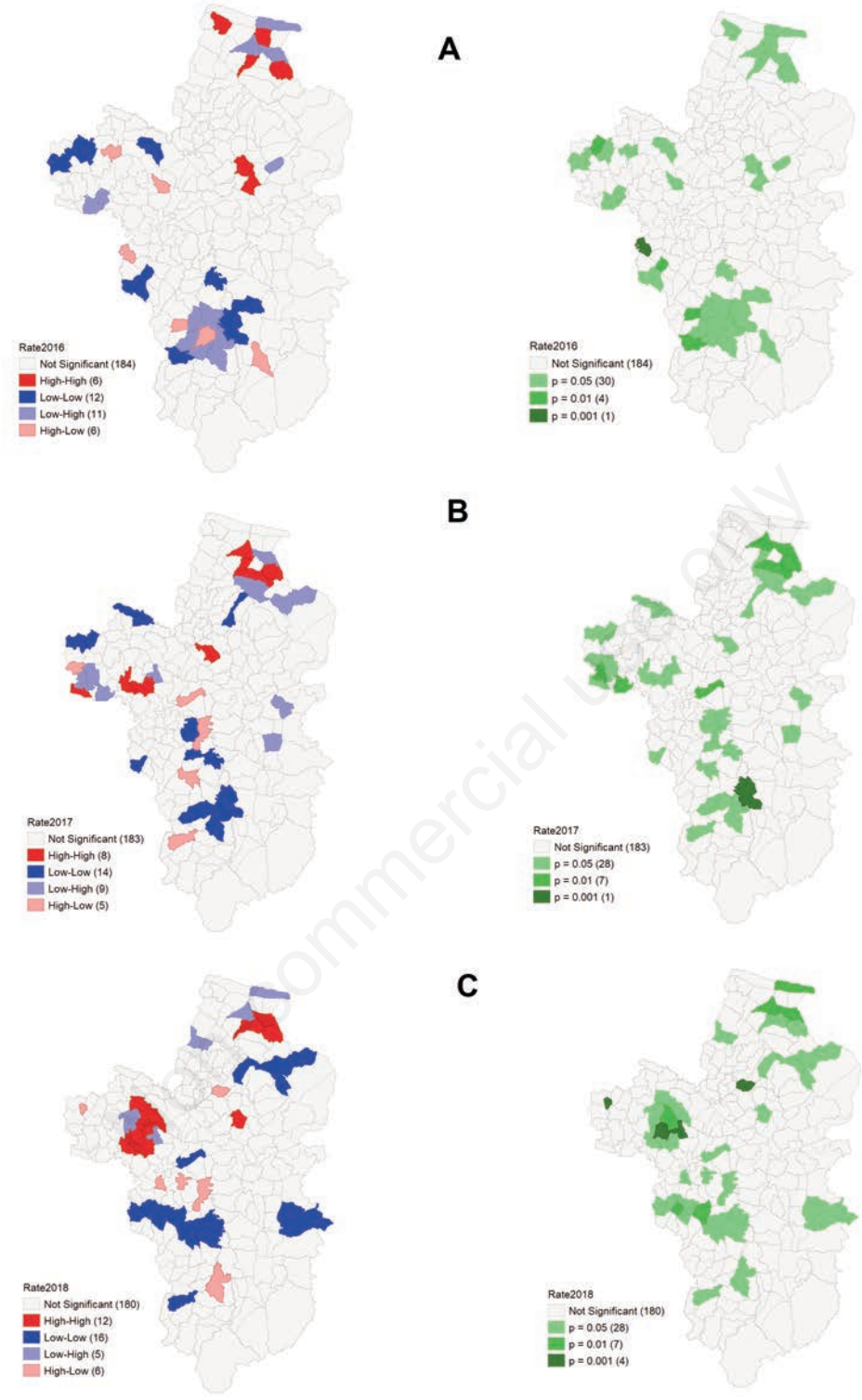

Figure 4. Spatial autocorrelation of melioidosis incidence in 2016-2018. Left: Hotspots of melioidosis incidence. Right: Significance of melioidosis incidence. A) 2016; B) 2017; C) 2018.

Discussion

Melioidosis outbreaks persist in Thailand's Ubon Ratchathani Province, where the incidence of culture-confirmed melioidosis exceeded 5 cases per 100 000 people from 2012 to 2015 (Hantrakun *et al*., 2019). Our study presents the trend and spatiotemporal data for 2016-2020. Although the incidence peaked in 2016, there was only a slight decrease and outbreaks continue to occur in the study area. Melioidosis incidence is related to meteorological factors including rainfall, temperature and humidity; 80% of the cases are correlated with rainfall and occur particularly during the rainy season (Currie *et al*., 2021). Indeed, rainfall contributes to the presence of melioidosis in several tropical countries (Bulterys *et al*., 2018; Liu *et al*., 2015; Mu *et al*., 2014). However, no associations between melioidosis incidence and meteorological factors have been detected in our study area or in Kuala Lumpur, Malaysia (Sam *et al*., 2007; Wongbutdee *et al*., 2021).

The strategy for monitoring and preventing melioidosis remains unclear, which is the reason we applied local Moran's *I* to statistically identify hotspots, coldspots and spatial outliers. This tool effectively identifies clustered distributions among locations revealing that hotspots were clustered mostly in the northern region, with outliers sparely distributed in the central one and close to other groups. The hotspot clustering may reflect the distribution of geographic features such as soil texture and drainage. Sandy loam, clay, and clay loam soil are habitats of *B. pseudomallei*, which is consistent with observations made in agricultural field soils such as rice paddies (Kaestli *et al*., 2009; Nachiangmai *et al*., 1985; Paksanont *et al*., 2018; Palasatien *et al*., 2008). Our findings reveal that melioidosis incidence is heterogeneous and unstable. People who are at risk can be infected with *B. pseudomallei* during all seasons. Groups at risk should therefore avoid direct contact with the bacteria and use protective equipment such as gloves and boots during activities and wash immediately after exposure to reduce the risk of melioidosis. Various lifestyle factors may increase the risk of exposure to *B. pseudomallei*. This study revealed the location of high-risk areas for monitoring and can be used as reference for melioidosis prevention. Understanding its spatial clustering makes surveillance and control easier than if the infection were randomly distributed and dispersed. Armed with knowledge of which sub-districts exhibit highly clustered melioidosis distributions, the Tambon Health Promoting Hospital (the

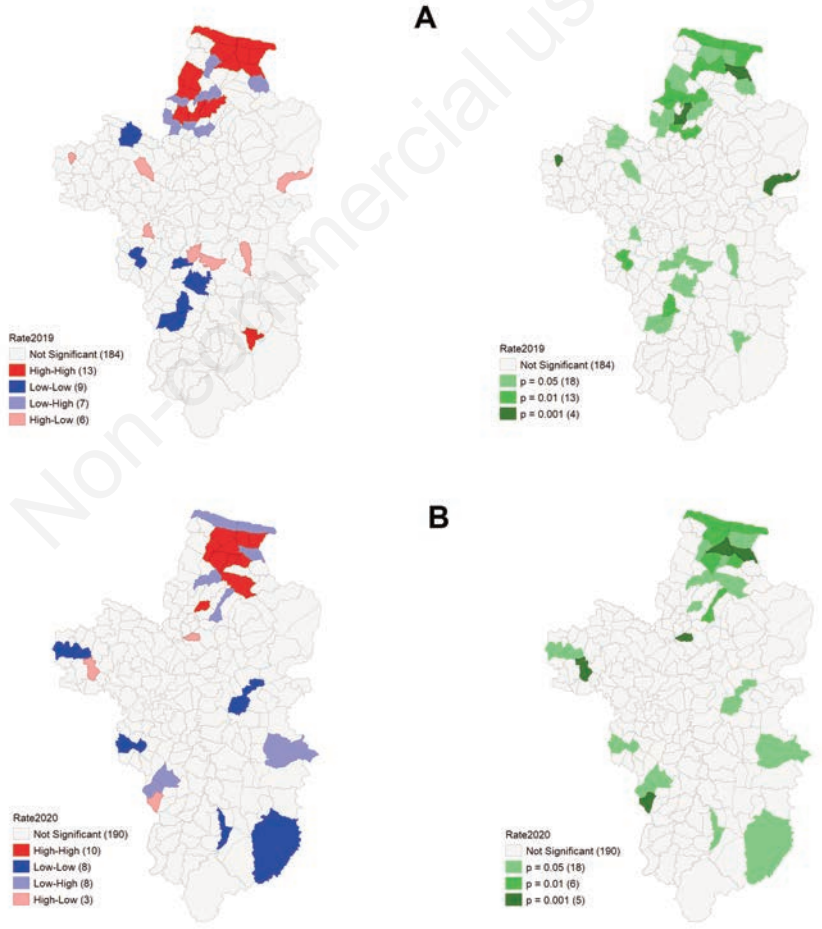

Figure 5. Spatial autocorrelation of melioidosis incidence in 2019-2020. Left: Hotspots of melioidosis incidence. Right: Significance of melioidosis incidence. A) 2019; B) 2020.

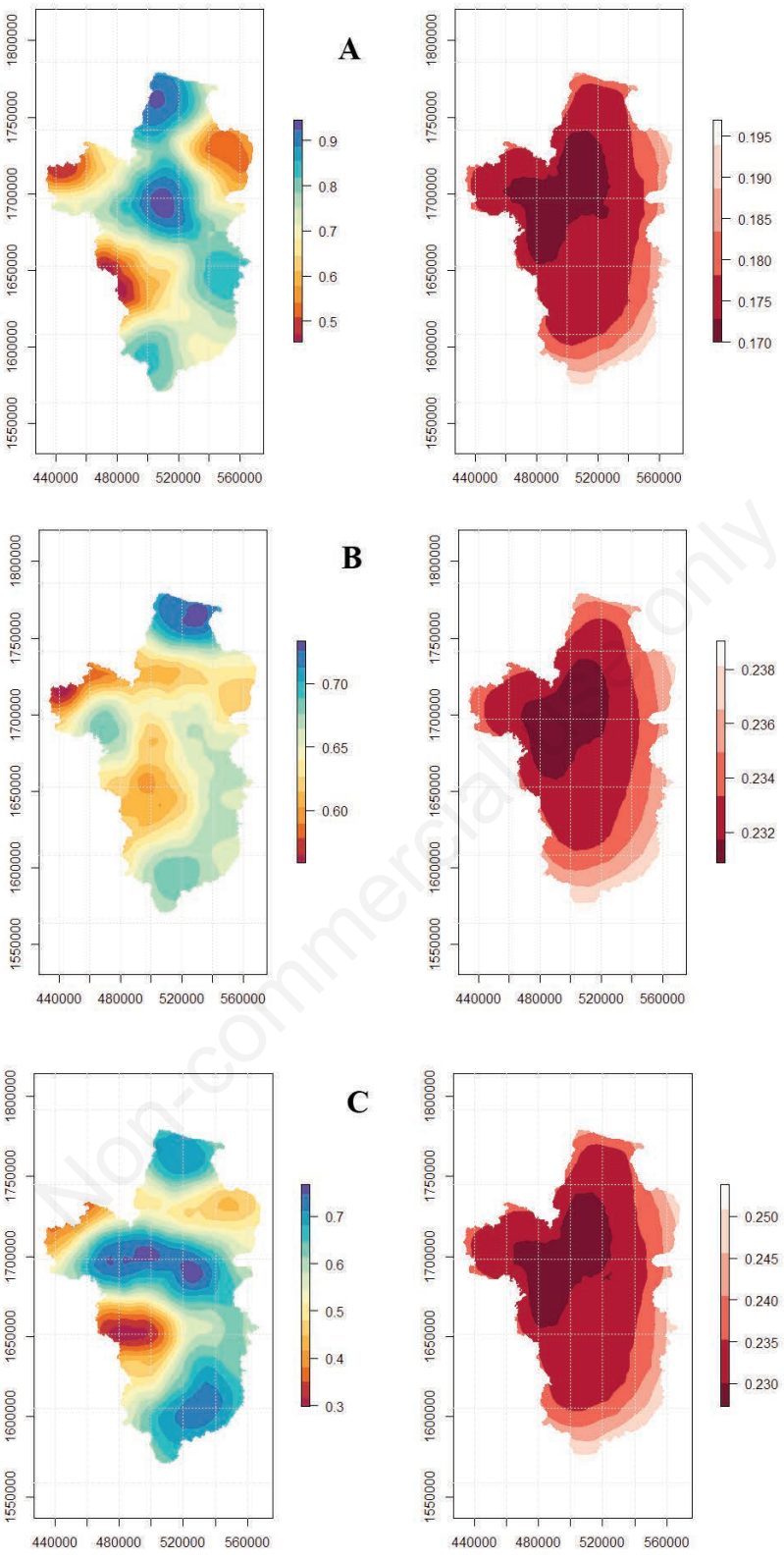

Figure 6. Maps of melioidosis incidence risk zonesin2016-2018. Left: Spatial predictions. Right: Variance. A) 2016; B) 2017; C) 2018.

primary health care provider for communities in each sub-district in Thailand) can now better address this issue. Health workers should be asked to promote activities to reduce risky perceptions and behaviours, creating healthy lifestyles that would minimize the incidence of this infection. Mapping of the melioidosis risk revealed the locations of melioidosis outbreaks each year. Although the northern region exhibits the highest risk of melioidosis outbreaks, indicating an increased risk of contracting *B. pseudomallei* from contaminated soil and water, the status of this bacterium in this area has not elucidated. It has been identified in the soil of rice fields in both Lao Suea Kok and Don Mod Deang districts (central region, Ubon Ratchathani), with positive spatial lag distances of 7.6 m (625 m^2) and 90.51 m (9.24 km^2), respectively (Limmathurotsakul *et al*., 2010; Saengnill *et al*., 2020). Here, however, we focused on a region where there is a high risk of *B. pseudomallei* contamination in both soil and water, which should improve the identification of high-risk zones and account for uncertainty regarding their distribution and size as well as reveal incidence clusters. They can thus be used by health workers for planning, prevention, disease control and resource allocation.

This research used sub-district level data that does not include the village level. Using village-level data weighting would generate different results. Adjacent regions are given more weight (and therefore influence) than more distant regions. As an alternative, space-time scanning can be applied to monitor disease outbreaks over time and obtain trends. Further, we used indicator Kriging, based on case reports to estimate the probability of melioidosis. Methods that account for environmental and climatic factors (including co-Kriging, regression Kriging, autoregressive and kernel density estimation) could also be used for spatial modelling of this disease risk.

Conclusions

Melioidosis severely and frequently affects the Ubon Ratchathani Province. Here, we used GIS to analyse the spatial distribution of melioidosis incidence and performed geostatistical prediction of the risk area. Melioidosis incidence was randomly distributed in 2016 but clustered in 2017–2020. The spatial distri-

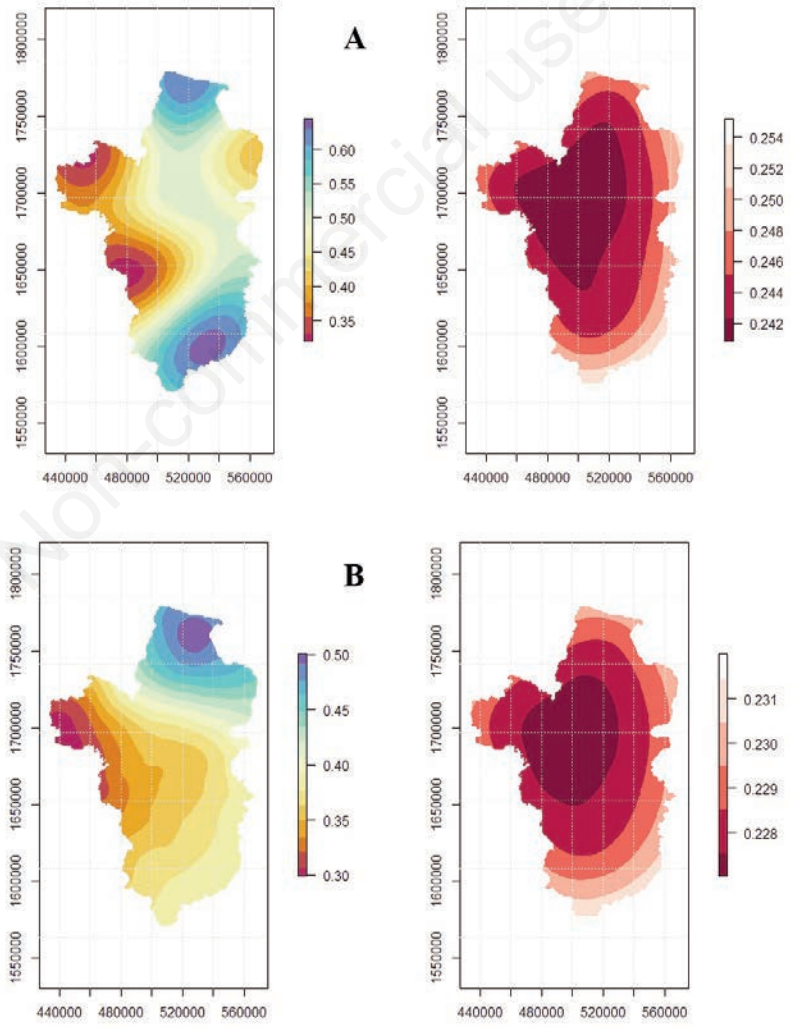

Figure 7. Maps of melioidosis incidence risk zones in 2019-2020. Left: Spatial predictions. Right: Variance. A) 2019; B) 2020.

bution reveals the annual locations of incidence, revealing high-risk areas and outliers adjacent to other groups. The northern region remains the highest risk area for melioidosis outbreaks, while outbreaks were sparse in the middle and southern regions. These findings provide a reference for reporting and decision-making for melioidosis surveillance and mitigation planning.

References

Bulterys PL, Bulterys MA, Phommasone K, Luangraj M, Mayxay M, Kloprogge S, Miliya T, Vongsouvath M, Newton PN, Phetsouvanh R, French CT, Miller JF, Turner P, Dance DAB. 2018. Climatic drivers of melioidosis in Laos and Cambodia: a 16-year case series analysis. Lancet Planet Health 2:e334-e343.

Bureau of Epidemiology, Department of Disease Control, MoPH, Thailand. 2023. National Disease Surveillance (Report 506): Melioidosis. Accessed January, 2023. Available from: http://doe.moph.go.th/surdata/disease.php?dcontent=old&ds=72

Chen YS, Lin HH, Mu JJ, Chiang CS, Chen CH, Buu LM, Lin YE, Chen YL. 2012. Distribution of melioidosis cases and viable Burkholderiapseudomallei in soil: evidence for emerging melioidosis in Taiwan. J Clin Microbiol 48:1432-4.

Corkeron ML, Norton R, Nelson PN. 2010. Spatial analysis of melioidosis distribution in a suburban area. Epidemiol Infect 138:1346-52.

Currie BJ, Ward L, Cheng AC. 2010. The epidemiology and clinical spectrum of melioidosis: 540 cases from the 20 year Darwin prospective study. PLoSNegl Trop Dis 4:e900.

Dai D, Chen YS, Chen PS, Chen YL. 2012. Case cluster shifting and contaminant source as determinants of melioidosis in Taiwan. Trop Med Int Health 17:1005-13.

Dance DAB, Luangraj M, Rattanavong S, Sithivong N, Vongnalaysane O, Vongsouvath M, Newton PN. 2018. Melioidosis in the Lao People's Democratic Republic. Trop Med Infect Dis 3:21.

Finkelstein RA, Atthasampunna P, Chulasamaya M. 2000. Pseudomonas (Burkholderia) pseudomallei in Thailand, 1964-1967: geographic distribution of the organism, attempts to identify cases of active infection, and presence of antibody in representative sera. Am J Trop Med Hyg 62:232-9.

GEODA software. Available from: https://gisgeography.com/geoda-software/

Han J, Zhu L, Kulldorff M, Hostovich S, Stinchcomb DG, Tatalovich Z, Lewis DR, Feuer EJ. 2016. Using Gini coefficient to determining optimal cluster reporting sizes for spatial scan statistics. Int J Health Geogr 15.

Hantrakun V, Kongyu S, Klaytong P, Rongsumlee S, Day NPJ, Peacock SJ, Hinjoy S, Limmathurotsakul D. 2019. Clinical Epidemiology of 7126 Melioidosis Patients in Thailand and the Implications for a National Notifiable Diseases Surveillance System. Open Forum Infect Dis 6:ofz498.

Kaestli M, Mayo M, Harrington G, Ward L, Watt F, Hill JV, Cheng AC, Currie B.J. 2009. Landscape Changes Influence the Occurrence of the Melioidosis Bacterium Burkholderia pseudomallei in Soil in Northern Australia. PLoS Negl Trop Dis 3:e364.

Kulldorff M. 1997. A spatial scan statistic. Communications in Statistics - Theory and Methods. 26:1481–1496.

Limmathurotsakul D, Kanoksil M, Wuthiekanun V, Kitphati R, Destavola B, Day NP, Peacock SJ. 2013. Activities of daily living associated with acquisition of melioidosis in northeast Thailand: a matched case-control study. PLoS Negl Trop Dis 7:e2072.

Limmathurotsakul D, Wongratanacheewin S, Teerawattanasook N, Wongsuvan G, Chaisuksant S, Chetchotisakd P, Chaowagul W, Day NP, Peacock SJ. 2010. Increasing incidence of human melioidosis in Northeast Thailand. Am J Trop Med Hyg 82:1113-7.

Limmathurotsakul D, Wuthiekanun V, Chantratita N, Wongsuvan G, Amornchai P, Day NP, Peacock SJ. 2010. Burkholderia-pseudomallei is spatially distributed in soil in northeast Thailand. PLoS Negl Trop Dis 4:e694.

Liu X, Pang L, Sim SH, Goh KT, Ravikumar S, Win MS, Tan G, Cook AR, Fisher D, Chai LY. 2015. Association of melioidosis incidence with rainfall and humidity, Singapore, 2003-2012. Emerg Infect Dis 21:159-62.

Mu JJ, Cheng PY, Chen YS, Chen PS, Chen YL. 2014. The occurrence of melioidosis is related to different climatic conditions in distinct topographical areas of Taiwan. Epidemiol Infect 142:415-23

Nachiangmai N, Patamasucon P, Tipayamonthein B, Kongpon A, Nakaviroj S. 1985. Pseudomonas pseudomallei in southern Thailand. Southeast Asian J Trop Med Public Health 16:83-7.

Paksanont S, Sintiprungrat K, Yimthin T, Pumirat P, Peacock SJ, Chantratita N. 2018. Effect of temperature on Burkholderia pseudomallei growth, proteomic changes, motility and resistance to stress environments. Scientific Reports 8:9167.

Palasatien S, Lertsirivorakul R, Royros P, Wongratanacheewin S, Sermswan RW. 2008. Soil physicochemical properties related to the presence of Burkholdoria pseudomallei. Trans R Soc Trop Med Hyg 102(Suppl 1): S5-9.

QGIS. Available from: https://qgis.org/

R gstat package. Available from: https://cran.r-project.org/web/packages/gstat/index.html

Rachlin A, Luangraj M, Kaestli M, Rattanavong S, Phoumin P, Webb JR, Mayo M, Currie BJ, Dance DAB. 2020. Using Land Runoff to Survey the Distribution and Genetic Diversity of Burkholderiapseudomallei in Vientiane, Laos. Appl Environ Microbiol 87:e02112-20.

Saengnill W, Charoenjit K, Hrimpeng K, Jittimanee J. 2020. Mapping the probability of detecting Burkholderiapseudo-mallei in rural rice paddy soil based on indicator kriging and spatial soil factor analysis. Trans R Soc Trop Med Hyg 114:521-530.

Sam IC, Puthucheary SD. 2007. Melioidosis and rainfall in Kuala Lumpur, Malaysia. J Infect 54:519-20.

Thaipadungpanit J, Chierakul W, Pattanaporkrattana W, Phoodaeng A, Wongsuvan G, Huntrakun V, Amornchai P, Chatchen S, Kitphati R, Wuthiekanun V, Day NP, Peacock SJ, Limmathurotsakul D. 2014. Burkholderia pseudomallei in water supplies, southern Thailand. Emerg Infect Dis 20:1947-1949.

Wang-Ngarm S, Chareonsudjai S, Chareonsudjai P. 2014. Physicochemical factors affecting the growth of Burkholderiapseudomallei in soil microcosm. Am J Trop Med Hyg 90:480-5.

Wongbutdee J, Saengnill W, Jittimanee J, Panomket P, Saenwang P. 2021. The association between the mapping distribution of melioidosis incidences and meteorological factors in an endemic area: Ubon Ratchathani, Thailand (2009–2018). CMU J Nat Sci 20:e2021083.